

PAPER

Fast MIMO Channel Calculation Technique for Multi-Antenna System Using Signal Modulation for FDTD Method

Kazuma OUCHIDA[†], *Student Member*, Naoki HONMA^{†a)}, and Yoshitaka TSUNEKAWA[†], *Members*

SUMMARY This paper proposes a new method that combines signal modulation and FDTD (Finite-Difference Time-Domain) simulations to reduce the computation time in multiple-antenna analysis. In this method, signals are modulated so as to maintain orthogonality among the excited signals; multiple antennas are excited at the same time. This means just one FDTD simulation is needed whereas the conventional method demands as many simulations as there are transmitting antennas. The simulation of a 2×2 multi-antenna system shows that the proposed method matches the performance of the conventional method even though its computation time is much shorter.

key words: FDTD, signal modulation, channel capacity, multi-antenna, MIMO

1. Introduction

Technologies for enhancing the data rate of wireless communication are being actively pursued, and diversity antenna [1] and Multiple-Input Multiple-Output (MIMO) systems [2] are seen as key advances. The characteristics of the multiple antennas greatly impact the diversity gain or channel capacity. The effect of the antenna characteristics on the MIMO channel was generalized by Wallace et al. [3], but the performance of a MIMO system strongly depends on the interaction between the antenna system and propagation environment. Therefore, evaluating a multiple antenna system still demands extensive simulations to fully elucidate the interaction. This incurs very high computation cost even with the recent progress in computers. Hence, an efficient method of MIMO channel simulation is needed.

The ray-tracing method [4]–[6] and the FDTD (Finite-Difference Time-Domain) method [7], [8] are currently being used to evaluate propagation characteristics. Since the ray-tracing method is based on geometric optics theory, highly complex structures explode the computation time and degrade analysis accuracy. The FDTD method, on the other hand, divides the analysis region into small cells, and Maxwell's equations are applied to explain the electromagnetic interactions among the cells. The FDTD method is convenient for analyzing detailed structures including the antennas and propagation environments. For this reason, many large scale analyses have been based on the FDTD method [8]. Unfortunately, its calculation time and memory requirement increase in proportion to the total volume of the

analysis space.

Fast FDTD analysis methods such as ADI (Alternating-Direction Implicit) method [9] and sub-cell method [10] have been proposed. In the ADI-FDTD method, the time step is not restricted by the CFL (Courant-Friedrichs-Lewy) condition. This method can reduce the computation time by setting large time steps as appropriate. On the other hand, the sub-cell method can deal with geometries that do not suit the cells used. Since there is no need to use fine cells throughout the entire analysis region, it can reduce both computation memory and time. Even though these techniques are effective in alleviating the computation load, analyzing an array antenna with a voluminous propagation environment needs long computation time that is proportion to the number of the antennas since each antenna needs to be excited individually. For this reason, a fast FDTD analysis suitable for multiple-antenna systems is required.

A fast analysis method for multiple-antenna systems using OFDM (Orthogonal Frequency Division Multiplexing) has been proposed [11]. This method enables the simultaneous analysis of multiple antennas since the excitation signals are spectrally orthogonalized by exploiting OFDM modulation. However, this method cannot analyze two channels with the same frequency and so the frequency response is intermittent.

To resolve this drawback, we proposed a fast analysis method using the spread spectrum technique [12], [13]. This method enables the simultaneous analysis of multiple antennas since the excitation signals are orthogonalized by exploiting non-identical spreading codes. However, the wide band signals generated by spreading codes average the frequency characteristics of the channel, and the accurate channel response at the specific frequency cannot be observed. Otherwise, a long period of the signal is needed for a high spectral resolution [14], but this causes serious increase in the FDTD time step. Therefore, neither this method nor [11] can analyze the MIMO channel in a multipath environment.

In this paper, we propose a fast analysis method for the multi-path environment. Its key advance is to introduce signal modulation to FDTD analysis. The modulated signals for multiple transmitting antennas are made orthogonal to each other, so the signals can be well separated (isolation is high) at the receiving antennas. That is, the multiple transmitting antennas are excited simultaneously and the MIMO channel can be calculated with just one simulation. The remainder of this paper describe the proposed scheme and mechanism in detail. Numerical analysis results are also de-

Manuscript received February 23, 2015.

Manuscript revised June 10, 2015.

[†]The authors are with the Graduate School of Engineering, Iwate University, Morioka-shi, 020-8551 Japan.

a) E-mail: honma@m.ieice.org

DOI: 10.1587/transcom.E98.B.2300

scribed; they show that the proposed method offers much faster analysis than the FDTD method with the conventional Gaussian pulse but with slight loss of accuracy.

2. The Concept of the Proposed Method

Figure 1 shows the concept of the proposed FDTD analysis method. In the FDTD method, the propagation channel is calculated using the voltage and current at the port of the receiving antenna. The total voltage and current in the time domain can be calculated first. After that, the voltage and current waveform in the time domain are transformed into frequency domain values by Fourier transformation. The channel is obtained from the voltage and current in the frequency domain. Figure 2 shows the transmitting and receiving ports. The transmitted signal vector and the received signal vector in the frequency domain are expressed as,

$$\mathbf{x} = \frac{1}{2}(\mathbf{v}_T/Z_0^{1/2} + \mathbf{i}_T Z_0^{1/2}) \tag{1}$$

$$\mathbf{y} = \frac{1}{2}(\mathbf{v}_R/Z_0^{1/2} - \mathbf{i}_R Z_0^{1/2}), \tag{2}$$

where Z_0 is the reference impedance used to define the scattering parameters. $\mathbf{v}_T = [v_{T1}, \dots, v_{TM_t}]$ and $\mathbf{v}_R = [v_{R1}, \dots, v_{RM_r}]$ are voltage vectors in the frequency domain at the port of the transmitting and receiving antenna, respectively. $\mathbf{i}_T = [i_{T1}, \dots, i_{TM_t}]$ and $\mathbf{i}_R = [i_{R1}, \dots, i_{RM_r}]$ are current

vectors in the frequency domain at the port of the transmitting and receiving antenna, respectively. Next, each of the transmitted signals is defined by the plurality of symbols $\mathbf{V} = [\mathbf{v}_{T1}, \dots, \mathbf{v}_{TN}]$. The transmitted signal vector is calculated by (1), and the transmitted signal matrix $\mathbf{X} = [\mathbf{x}_1, \dots, \mathbf{x}_N]$ is generated. The number of transmitted symbols, N , is made equal to the number of transmitting antennas. The transmitted symbol length is T [time step]. Then in the time domain, guard times, G_t , are inserted between each of the transmitted symbols to prevent inter-symbol interference at the receiver due to multi-path delay spread in the radio channel. All antennas are excited at the same time by these signals. On the receiving side, the received signal vector is calculated by (2), and the received signal matrix $\mathbf{Y} = [\mathbf{y}_1, \dots, \mathbf{y}_N]$ is generated. The MIMO channel is calculated by

$$\mathbf{H} = \mathbf{Y}\mathbf{X}^{-1}. \tag{3}$$

3. Numerical Results

3.1 Analysis Condition

The numerical analysis model of this study assumes dipole arrays, see Fig. 3. In order to evaluate the MIMO channel in a multi-path environment, the dipole arrays are surrounded by concrete walls, one of which is pierced by a large window. Two types of multi-path environments, i.e. line-of-sight (LOS) and non-line-of-sight (NLOS), are evaluated in this study. Both models are identical except for

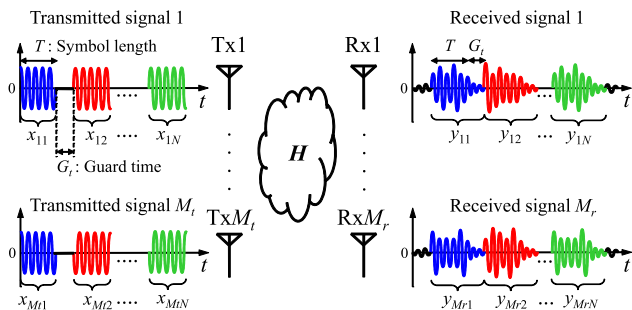


Fig. 1 Concept of the proposed method.

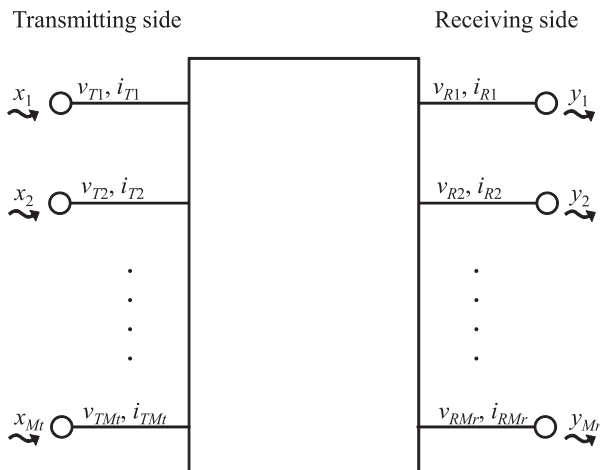
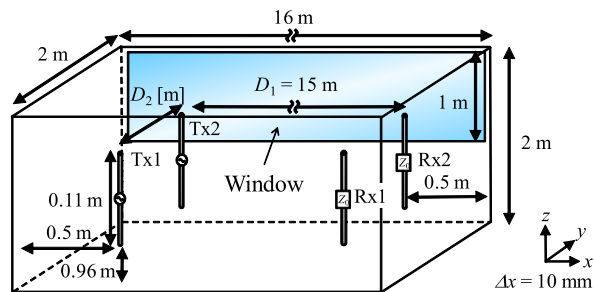
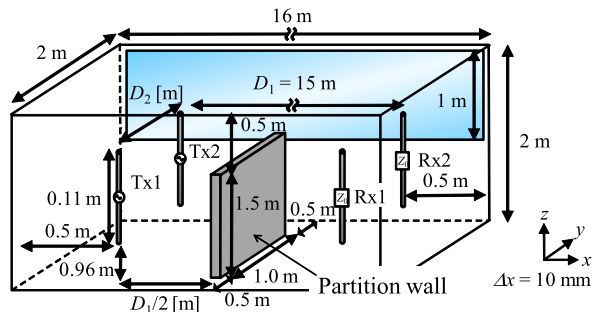


Fig. 2 Transmitting and receiving ports.



(a) LOS model



(b) NLOS model

Fig. 3 Analysis model.

Table 1 Parameters of the structures.

	Wall	Window
Relative permittivity ϵ_r	5.5 [15]	7.2
Relative permeability μ_r	1	1
Electrical conductivity σ	0.023	0.0293
Thickness	60 mm	10 mm

Table 2 Parameters for analysis.

Antenna	Dipole antenna
Feeding model	Delta-gap feed
Cell size	10 mm
Absorbing B.C.	PML
Number of PML layer	8
Analysis frequency	1.125 GHz
Time step	19.26 ps

a partition wall between transmitting and receiving arrays. The partition wall is located at the center of the room to block the direct path between transmitting and receiving arrays for NLOS model. Parameters of the structures are summarized in Table 1. The distance between the transmitting and receiving antennas is D_1 [m], and element spacing is D_2 [m]. The distance between each element and the wall is 0.5 m. Details of the FDTD analysis configurations are summarized in Table 2. A Gaussian pulse and modulated signal pulse are used as the excitation signal. The latter is generated by BPSK (Binary Phase Shift Keying), and the excitation signal is given by

$$v_{Tlk}(t) = \sin[2\pi f\{t - (k-1)(T + G_t)\} + \theta_{lk}], \quad (4)$$

$$\theta_{lk} = 0, \pi. \begin{cases} l = 1, \dots, M_t \\ k = 1, \dots, N \end{cases} \quad (5)$$

θ_{lk} is determined to make the signal sets orthogonal to each other because the orthogonal signal sets offers high accuracy in the calculation (3). In the frequency domain, the signal set of k -th period can be expressed as,

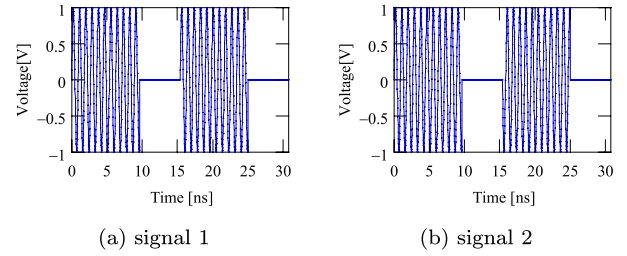
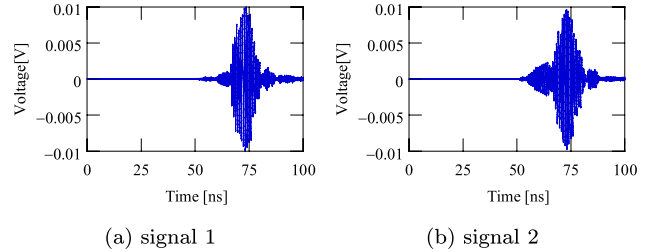
$$\mathbf{x}_k = \begin{pmatrix} x_{1k} \\ \vdots \\ x_{M_t k} \end{pmatrix} = \frac{j}{\sqrt{M_t}} \begin{pmatrix} \exp(j\theta_{1k}) \\ \vdots \\ \exp(j\theta_{M_t k}) \end{pmatrix}. \quad (6)$$

Therefore, the signal matrix can be written as,

$$\mathbf{X} = \begin{pmatrix} x_{11} & \cdots & x_{1N} \\ \vdots & \ddots & \vdots \\ x_{M_t 1} & \cdots & x_{M_t N} \end{pmatrix} = \frac{j}{\sqrt{M_t}} \begin{pmatrix} \exp(j\theta_{11}) & \cdots & \exp(j\theta_{1N}) \\ \vdots & \ddots & \vdots \\ \exp(j\theta_{M_t 1}) & \cdots & \exp(j\theta_{M_t N}) \end{pmatrix}. \quad (7)$$

In order to realize the orthogonality among the signal sets, the signal matrix, \mathbf{X} , needs to be unitary. Hence, θ_{lk} is chosen to satisfy the relation, $\mathbf{X}\mathbf{X}^H = \mathbf{I}$. As an example, the signal set for $M_t = 2$ is determined as,

$$\begin{pmatrix} \theta_{11} & \theta_{12} \\ \theta_{21} & \theta_{22} \end{pmatrix} = \begin{pmatrix} 0 & 0 \\ 0 & \pi \end{pmatrix}. \quad (8)$$

**Fig. 4** Modulated pulse waveforms.**Fig. 5** Received signal waveforms.

Therefore, the signal matrix is expressed as,

$$\mathbf{X} = \frac{j}{\sqrt{2}} \begin{pmatrix} 1 & 1 \\ 1 & -1 \end{pmatrix}. \quad (9)$$

which satisfies unitary condition and is used in the following analysis.

In this study, an in-house-developed FDTD code was used for both conventional and proposed analyses, where basic and standard FDTD algorithm written in FORTRAN 90 was used.

3.2 Channel Characterization with the Guard Time Length and Symbol Length

Figure 4 shows the modulated pulse waveforms. Antenna Tx1 transmits signal 1 shown in Fig. 4(a), and antenna Tx2 transmits signal 2 shown in Fig. 4(b). Here, the symbol length is set to $T = 500$ time steps, and the guard time length, G_t , is 300 time steps. In the proposed method, analyses that use modulated pulses require $2(T + G_t)$ [time steps] for excitation and analysis. This is because guard times are inserted between each of the transmitted symbols to prevent inter-symbol interference at the receiver that would otherwise be caused by multi-path delay spread.

Figure 5 shows received signal waveforms, which is the simulated in NLOS model (b). The distance between the transmitting and receiving antennas is $D_1 = 15$ m and element spacing is $D_2 = 0.1$ m. Antenna Rx1 received signal 1 is shown in Fig. 5(a), and antenna Rx2 received signal 2 is shown in Fig. 5(b). N_t must set so that the excitation signal reaches the receiving antenna, i.e.,

$$N_t = \frac{D_1}{v_c \Delta t}, \quad (10)$$

where v_c is the wave velocity in a vacuum, Δt is the time

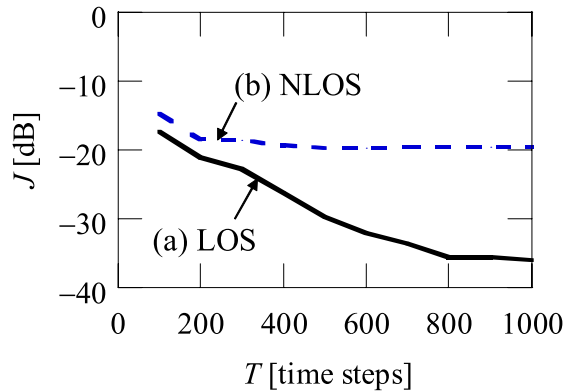


Fig. 6 Channel error versus symbol length.

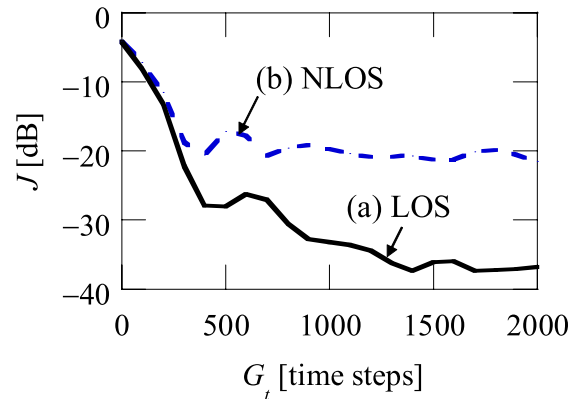


Fig. 7 Channel error versus guard time length.

step. Figure 5 shows that the propagation delay time is about 50 ns. This value is equal to the value calculated by (10).

Figure 6 plots channel error versus symbol length for LOS and NLOS cases. The channel error is defined as,

$$J = \frac{\|\mathbf{H}^{ref} - \mathbf{H}\|_F^2}{\|\mathbf{H}^{ref}\|_F^2}, \quad (11)$$

where \mathbf{H} is the propagation channel to be evaluated, and \mathbf{H}^{ref} is the propagation channel obtained by the Gaussian pulse with sufficiently long time analysis (10000 time steps). In the method using a modulated signal, the number of time steps required for the analysis is given by,

$$N_{total} = N_t + 2(T + G_t), \quad (12)$$

where T is the length of the excitation symbol and G_t is the length of the guard time. In this simulation, $G_t = 300$ time steps. The symbol length, T , is changed from 100 to 1000 time steps. The distance between the transmitting and receiving antennas is $D_1 = 15$ m, and element spacing is $D_2 = 0.1$ m. The results in Fig. 6 show that increasing the symbol length decreases the channel errors. This also shows that the error in NLOS environment is remaining even when the symbol length is increased whereas that in LOS decreases with symbol length. It is considered that the power of the direct path is dominant and the power of the delayed multipath component is almost negligible in LOS environment. Nevertheless, the error at $T > 200$ time steps is lower than -15 dB for both environments.

Figure 7 shows channel error versus guard time length. In this simulation, $T = 256$ time steps. The guard time length, G_t , is changed from 0 to 2000 time steps. Even though the error in NLOS environment is larger than that of the LOS environment, the sufficiently long guard time offers fairly accurate results. It is found that the proposed method can analyze the MIMO channel if the guard time length is about half the delay spread, which was about 40 ns (2000 time steps). Here, this delay spread is fairly typical for small indoor environment at this frequency band [16].

From the results shown here, it is found that NLOS environment yields larger error than LOS environment. Since the accuracy for LOS is obviously higher than that of LOS,

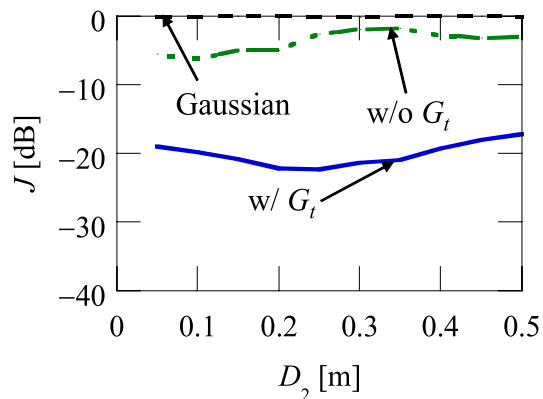


Fig. 8 Channel error versus element spacing.

NLOS environment is evaluated in the following discussion.

3.3 Comparison with the Conventional Method

Figure 8 shows channel error versus element spacing, where the error is the channel difference from the result with Gaussian pulse with long calculation time and is defined by (11). The results obtained by the proposed method are compared to the results obtained by the conventional method. Here, the number of time steps, N_{total} , is 5300. In the analysis using the Gaussian pulse, two individual analyses for two antennas are performed. In order to equalize the total calculation time, the number of time steps for Gaussian pulse is set to $N_{total}/2 = 2650$ time steps. ‘w/o G_t ’ shows the results for the case of not inserting a guard time. In this simulation, $T = 256$ and $G_t = 1000$ time steps. The output of conventional method without Gaussian pulse contains large error. The reason is the propagation time between the transmitting and receiving antennas. Since the signal transmitted from one antenna cannot reach the other antenna, the channel cannot be calculated correctly. The results for the case of not inserting a guard time, large error due to inter-symbol interference is present. However, the proposed method can analyze the two antennas at once, and the channels obtained by the proposed method agree very well.

Figure 9 shows Signal-to-Noise Ratio (SNR) versus el-

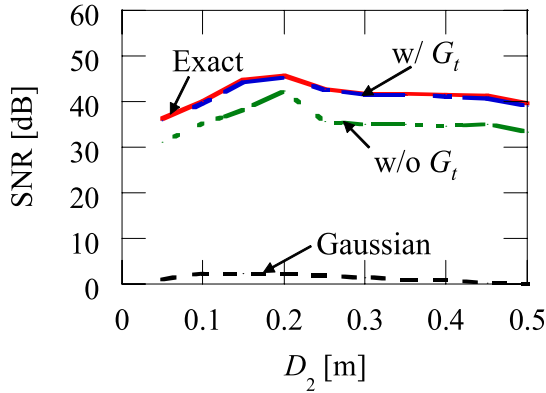


Fig. 9 SNR versus element spacing.

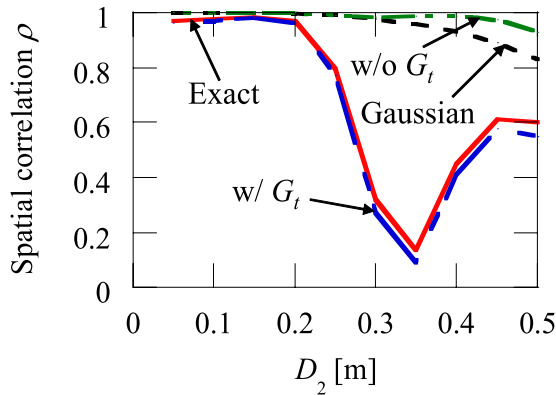


Fig. 10 Spatial correlation versus element spacing.

ement spacing. The SNR is given by

$$\text{SNR} = 10 \log_{10} \left[\frac{\text{Tr}(\mathbf{H}\mathbf{H}^H)\mathbf{P}}{M_t M_r \sigma^2} \right] \text{ [dB]}, \quad (13)$$

where, P is the transmission power and σ^2 is the noise power. In this simulation, transmission power is 0 dBm, and noise power is -80 dBm. ‘Exact’ shows the SNR obtained by a long time (10000 time steps) calculation with the Gaussian pulse. The SNR obtained by the proposed method agrees very well with the exact result. However, it is seen that SNR of the conventional method is about 40 dB.

Figure 10 plots spatial correlation versus element spacing. It is seen that the difference between ‘Exact’ and the proposed method is about 0. However, large error is present with the results corresponding to w/o G_t and Gaussian pulse. As discussed in Fig. 8, the delayed multipath components cause inter-symbol-interference, and the channel cannot be estimated correctly for w/o G_t . In conventional method, the physical time in the simulation is not sufficient for the signal reaching the receiving antennas, and the channel cannot be calculated correctly, too.

Figure 11 plots channel capacity versus element spacing. The channel capacity is obtained as

$$C = \log_2 \left[\det \left(\mathbf{H}\mathbf{H}^H \frac{P}{M_t \sigma^2} + \mathbf{I} \right) \right] \text{ [Bits/s/Hz]}, \quad (14)$$

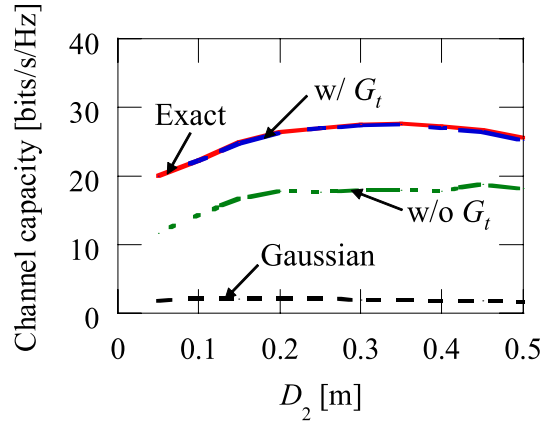


Fig. 11 Channel capacity versus element spacing.

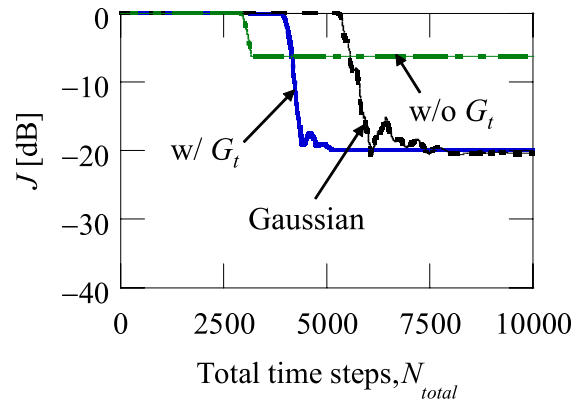


Fig. 12 Channel error versus total time steps.

where, transmission power is 0 dBm, and noise power is -80 dBm. The channel capacities obtained by the proposed method agree very well with the exact result. However, it is seen that channel capacities of the conventional method are about 20 bits/s/Hz.

3.4 Comparison of the Analysis Time Required

We compared the analysis time required by the proposed method to that by the conventional method.

Figure 12 plots channel error versus total time steps. Here, the distance between the transmitting and receiving antennas is $D_1 = 15$ m, and element spacing is $D_2 = 0.1$ m. The symbol length, T , is 256 time steps, and guard time length, G_t , is 1000 time steps. Large error is present in the Gaussian pulse results when the total time steps, N_{total} is about 5000. On the other hand, the channel error of the proposed method is only -20 dB or so. For the channel error of -15 dB, the proposed method needed 4305 time steps, while the conventional method with Gaussian pulse took 5883 time steps. Therefore, the proposed method could reduce the computation time by 26%. Note that the CPU time of post processing for channel estimation is negligible compared to the FDTD simulation. In this study, a PC with Intel Core i7 980X Extreme Edition and 24 GB memory was

used. A single-core compiler was used and the CPU time for the model shown in Fig. 3 with 10000 time steps was 13,023 seconds.

4. Conclusion

This paper presented a fast FDTD analysis method for multiple-antenna systems that uses signal modulation. The modulation ensures orthogonality among the excited signals. Simulations showed that the proposed method yields channel characteristics that agree well with those of the conventional method even though it reduces the computation time by about 26%. Simulation of a small scale system, 2×2 antennas, demonstrated that our analysis method is effective in reducing the computation time of FDTD analysis of multiple-antenna systems while offering acceptable accuracy.

As a final remark, the proposed method can be applied to array antenna systems that have arrays larger than 2×2 . Nevertheless, the increase of the transmitting antennas causes the interference among the signals larger than that of the 2×2 case. This means the quantitative studies on the signal parameters, such as the length of the guard and symbol, and so on, are needed. This issue will be investigated and presented in our future works.

Acknowledgements

This research was partially supported by JSPS KAKENHI (25709030).

References

- [1] J.H. Winters, J. Salz, and R.D. Gitlin, "The impact of antenna diversity on the capacity of wireless communication systems," *IEEE Trans. Commun.*, vol.42, pp.1740–1751, Feb. 1994.
- [2] G.J. Foschini and M.J. Gans, "Capacity when using diversity at transmit and receive sites and the Rayleigh-faded matrix channel is unknown at the transmitter," *Proc. WINLAB Workshop on Wireless Information Network*, vol.435, pp.253–267, March 1996.
- [3] J.W. Wallace and M.A. Jensen, "Mutual coupling in MIMO wireless systems: A rigorous network theory analysis," *IEEE Trans. Commun.*, vol.3, no.4, pp.1317–1325, July 2004.
- [4] J.W. McJown and R.L. Hamilton, Jr., "Ray tracing as a design tool for radio networks," *IEEE Network Magazine*, vol.5, no.6, pp.27–30, Nov. 1991.
- [5] G. Lampard and T. Vu-Dinh, "The effect of terrain on radio propagation in urban microcells," *IEEE Trans. Veh. Tech.*, vol.42, no.3, pp.314–317, Aug. 1993.
- [6] T. Imai and T. Fujii, "Propagation loss in multiple diffraction using ray-tracing," 1997 *Antennas and Propagation Society International Symposium (APS 1997)*, Proc. APS'97, vol.4, pp.2572–2575, July 1997.
- [7] K.S. Yee, "Numerical solution of initial boundary value problems involving Maxwell's equations in isotropic media," *IEEE Trans. Antennas Propag.*, vol.AP-14, no.3, pp.302–307, May 1966.
- [8] T. Hikage, T. Nojima, S. Watanabe, and T. Shinozuka, "Electric-field distribution estimation in a train carriage due to cellular radios in order to access the implantable cardiac pacemaker EMI in semi-echoic environments," *IEEE Trans. Commun.*, vol.E88-B, no.8, pp.3281–3286, Aug. 2005.
- [9] T. Namiki and K. Ito, "Investigation of numerical errors of the two-dimensional ADI-FDTD method," *IEEE Trans. Microwave Theory and Tech.*, vol.48, no.11, pp.1950–1956, Nov. 2000.
- [10] J.J. Boonzaaier and C.W.I. Pistorius, "Thin wire dipoles a finite-difference time-domain approach," *Electronics Letters*, vol.26, no.22, pp.1891–1892, 1990.
- [11] M. Obara, N. Honma, Y. Suzuki, "Fast S-parameter calculation technique for multi-antenna system using temporal-spectral orthogonality for FDTD method," *IEICE Trans. Commun.*, vol.E95-B, no.4, pp.1338–1344, April 2012.
- [12] K. Ouchida, N. Honma and Y. Tsunekawa, "Fast FDTD analysis of MIMO channel using spread spectrum technique," 2013 *Asia-Pacific Microwave Conference (APMC 2013)*, Electric Proc. APMC 2013, T3D-1, pp.389–391, Nov. 2013.
- [13] K. Ouchida, N. Honma, and Y. Tsunekawa, "Fast MIMO channel calculation technique for multi-antenna system using spread spectrum technique for FDTD method," *IEICE Communications Express*, vol.3, no.3, pp.104–109, March 2014.
- [14] J.D. Parsons, D.A. Demery, and A.M.D. Turkmani, "Sounding techniques for wideband mobile radio channels: A review," *IEE Proceedings*, vol.138, no.5, pp.437–446, 1991.
- [15] Y. Yamaguchi, T. Abe, T. Sekiguchi, and J. Chiba, "Attenuation constants of UHF radio waves in arched tunnels," *IEEE Trans. Microwave Theory Tech.*, vol.33, pp.714–718, Aug. 1985.
- [16] A.A. Saleh and R.A. Valenzuela, "A statistical model for indoor multipath propagation," *IEEE J. Select. Areas Commun.*, vol.5, pp.128–137, Feb. 1987.



Kazuma Ouchida received the B.E. in electrical and electronic engineering from Iwate University, Morioka, Japan in 2013. He is currently with East Japan Railway Company. He received the APMC Best Student Paper Award in 2013.



Naoki Honma received the B.E., M.E., and Ph.D. degrees in electrical engineering from Tohoku University, Sendai, Japan in 1996, 1998, and 2005, respectively. In 1998, he joined the NTT Radio Communication Systems Laboratories, Nippon Telegraph and Telephone Corporation (NTT), in Japan. He is now working for Iwate University. He received the Young Engineers Award from the IEICE of Japan in 2003, the APMC Best Paper Award in 2003, the Best Paper Award of IEICE Communication Society in 2006, and the APMC2014 Prize in 2014, respectively. His current research interest is MIMO antenna system and its applications. He is a member of IEEE.



Yoshitaka Tsunekawa received the B.E. degree from Iwate University, Morioka, Japan, in 1980 and the M.E. and the Doctor of Engineering degrees from Tohoku University, Sendai, Japan, in 1983 and 1993, respectively. Since 1983, he has been with the Faculty of Engineering, Iwate University, where he is now a professor at the Department of Electrical Engineering and Computer Science. His current research interests include digital signal processing and digital control. He is a member of the Institute

of Electronics, Information and Communication Engineers of Japan, and IEEE.